A 3D GEOPHYSICAL MODEL OF THE CRUST IN THE BARENTS SEA REGION: MODEL CONSTRUCTION AND BASEMENT CHARACTERIZATION

Oliver Ritzmann[1], Nils Maercklin[2], Jan Inge Faleide[1,2],
Hilmar Bungum[1,2], Walter D. Mooney[3], and Shane T. Detweiler[3]

University of Oslo[1], NORSAR[2], and U.S. Geological Survey[3]

Sponsored by National Nuclear Security Administration
Office of Nonproliferation Research and Development
Office of Defense Nuclear Nonproliferation

Contract No. DE-A104-2000AL66517[1,2,3]

ABSTRACT

We here present BARENTS50, a new 3D geophysical model of the crust in the Barents Sea region. The target region of interest comprises northern Norway and Finland, parts of the Kola Peninsula and the East European lowlands. Novaya Zemlya, the Kara Sea and Franz-Josef Land terminate the region to the east, while the Norwegian-Greenland Sea marks the western boundary. In total, 680 one-dimensional seismic velocity profiles were compiled, mostly by sampling 2D seismic velocity transects, from seismic refraction profiles, every 25 km. Seismic reflection data in the western Barents Sea were further used for density modeling and subsequent density-to-velocity conversion. Velocities from these profiles were binned into two sedimentary and three crystalline crustal layers. The first step of the compilation comprised the layer-wise interpolation of the velocities and thicknesses. Within the different geological provinces of the study region, linear relationships between the thickness of the sedimentary rocks and the thickness of the remaining crystalline crust are observed. We therefore used the separately compiled (area-wide) sediment thickness data to adjust the crystalline crustal thickness according to the sedimentary thickness where no constraints from 1D velocity profiles existed. The BARENTS50 model is based on an equidistant hexagonal grid with a node spacing of 50 km. The P-wave velocity model was used for gravity modeling in order to obtain 3D density structure in the study region. A better fit to the observed gravity was achieved using a grid search algorithm which focused on the density contrast of the sediment-basement interface. The high resolution of 50 km is an improvement compared to older geophysical models. The BARENTS50 model is available at http://www.norsar.no/barents3d.

OBJECTIVES

We provide a new, high-resolution 3D geophysical model of the Barents Sea region, including Novaya Zemlya, using an updated data compilation. Our model aims to be precise enough both for further basic geological research and for the detection, location and characterization of small events in the greater Barents Sea region.

RESEARCH ACCOMPLISHED

Three-dimensional seismic models of the Earth's crust and mantle play important roles in the detection and classification of seismic events. Seismic waves which cross the Moho discontinuity experience traveltime delays, since the crust has relatively low seismic velocities compared to the upper mantle. The crustal structure often contains inhomogeneities such as sedimentary basins with very low seismic velocities. Accurate velocity models of the crust and upper mantle are therefore required tools for seismic event detection, location, discrimination, source inversion and for subsequent traveltime modeling. Once a 3D model is extended by the addition of other physical rock properties, such as the S-wave velocity, the density structure or the Q-structure, it will also provide general capabilities for lithological and geological interpretations.

Previously, velocity models were developed at a variety of scales, such as local, regional, plate, or global scales. They were based on numerous methods of study, such as body and surface-wave tomography, receiver function analysis, thermodynamic modeling or, as carried out here, by compiling first-order velocity data from active seismic refraction experiments. The data coverage eventually limits the model quality, and crustal seismic experiments are mostly distributed unevenly. The velocity compilation for the Barents Sea region, as documented in this paper, is based on a large amount of first-order data (Figure 1).

Global-scale seismic models reveal resolutions of 0.5º to 5º constructed along the Earth's longitude-latitude geographical grid. This configuration is particularly problematic at high latitudes since poor data coverage contrasts with the large number of grid nodes. We therefore chose to use an equidistant grid with a node spacing of 50 km to exploit the input data properly.

The compilation strategy for the BARENTS50 model has been as follows: We collected all available velocity data based on seismic refraction experiments in the target region. A number of profiles were obtained during this study from density modeling along deep seismic reflection profiles and subsequent density-to-velocity conversion. Subsequently, the seismic velocities and layer thicknesses were interpolated layer-by-layer. We observed different linear relationships between the sediment thickness and the thickness of the crystalline crust in the different provinces of our target region. A compiled sediment thickness map was used to adjust the crystalline crustal thicknesses where no database constraints were given. The 3D velocity structure was then converted into density and used for gravity modeling, in order to obtain the 3D density structure. A programmed grid search algorithm helped to obtain a better fit to the observed gravity field. The 3D model of Levshin et al. (2005) was used to extend our model into the upper mantle. The S-wave structure for the crustal section was estimated using crustal P/S-wave ratios from same model.

In order to demonstrate the improvements of the newly developed BARENTS50 model we have compared it to commonly applied 3D models. To this end, Figure 2 shows the (one-way) traveltimes of seismic P-waves from sea level down to the Moho discontinuity in comparison to 3SMAC (Nataf & Ricard, 1996), CRUST2.0 (Bassin et al., 2000) and WENA1.0 (Pasyanos et al., 2004). These illustrations represent roughly the expected traveltime delay for incoming seismic waves, caused by the relatively low seismic velocities of the crust compared to the mantle. The most significant improvement is the increased resolution of 50 km (Fig. 2a) compared to the very smooth fields derived from other models. Generally, the defined geological provinces have a strong effect on the traveltime distribution. Strong gradients in the traveltime are achieved if neighboring provinces are very different in the calculated regression (Fig. 3). The large traveltime obtained at 73°N/40°E is located at a prominent change of the heading along the profile AR-1 by Sakoulina et al. (2003). This is the only location where the traveltime map (Fig. 2a) reflects the input data distribution (Fig. 1). Here, we did not adjust the crystalline crustal thicknesses, since nearby data constraints were given.

The western continent-ocean transition (COT) is clearly visible in the BARENTS50 model; here the traveltimes drop from ca. 5 to 4 s towards the west. The WENA1.0 (Fig. 2b) model shows the COT similar to our model,

although the Moho is about 1.0 s deeper. Local positive undulations in the traveltimes along the COT in the CRUST2.0 (Fig. 2c) model are most likely due to local deposition centers and high accumulation of glacial sediments, with no traveltime effect in the BARENTS50 model. The average traveltime in the western Barents Sea is about 5.0 s and slightly higher in the east (ca. 6.0-6.5 s; Fig. 2a). This trend is approximately matched by the CRUST2.0 model. The 3SMAC model is notable here, since a strong positive traveltime anomaly is located centrally on the Barents shelf (Fig. 2d). The Barents Sea is represented by a 1D structure in the WENA1.0 model so that local anomalies are absent. Onshore Fennoscandia, 3SMAC and CRUST2.0 match well the trend of lower traveltimes in the Caledonian Orogen and towards the Kola Peninsula; again, WENA1.0 incorporates an average model that does not account for regional features of 200-400 km width. Prominent differences between all models occur as well in the region of the Novaya Zemlya Fold Belt and the Kara Sea. While 3SMAC shows no N-S striking anomalies along Novaya Zemlya, the remaining models obviously account for the structure of the foldbelt. WENA1.0 shows a remarkably mismatch with a traveltime of more than 8 s due to a regional crust thickness of 47 km. Here, the differences are locally to more than 3.0 s.

Transects through the 3D velocity model reveal for the first time simplified geological sections through the European Arctic from the Norwegian-Greenland Sea, across the continental margin, to the Barents Sea, the Novaya Zemlya Foldbelt and into the Kara Sea region. The 3D construction of the sedimentary basins can be interpreted with the crystalline crustal units and Moho topography below. Depth to Moho is shown in Figure 4. With respect to the chosen approach of regionalization, most of the geological provinces reveal a homogenous crustal structure. Naturally, the denser the data coverage the more complex is the local structure of the model. The crustal construction is more differentiated and the Moho topography more pronounced in the west, where the majority of data constraints are provided. Here, the Paleozoic and Mesozoic rifting history in the western Barents Sea resulted in a complex array of basins and basement highs which supposedly are inherited from the Caledonian consolidation phase (Gudlaugsson et al., 1998).

A fundamental step during the velocity model compilation was the adjustment of the crustal thickness according to the linear and province-related relationships between the sediment thickness and the thickness of the remaining crust (Fig. 3). The fundamental consideration behind this approach is that subsidence and the development of sediment basins is coeval with the flexure and/or thinning of the underlain crust. Regional conditions, such as density of the crust and mantle, the strain and stress rates, the viscosity and strength of the crust and, obviously, the sediment supply result therefore in a specific (local) thickness relation between the sedimentary cover and the remaining crust. Simple models of crustal extension (e.g., McKenzie, 1978) show that after the cooling of the stretched lithosphere (>120 Ma) the relation between basin depth and crystalline crust follows a straight line similar to an Airy-type isostatic compensation model (e.g., Watts, 2001). Prior to the state of thermal equilibrium the ratio between basin depth (sediment thickness) and thinned crystalline crust is slightly curvilinear. If, for example, the density of the crust is increased, the straight lines get steeper slopes; similarly, we expect other regional parameters to contribute to the final trend of the relationship. The earliest rift period in the Barents and Kara Seas is supposed in late Cambrian times (510 Ma; O'Leary et al., 2004), while the latest phase of rift-related subsidence and deposition was in the Early Cretaceous (100 Ma; Faleide et al., 1993). Additional extension has also been suggested in Late Cretaceous-Early Cenozoic times, following the break-up along the western Barents Sea margin; nevertheless a straight or slightly curvilinear relationship can be expected.

Figure 3 shows, despite the scatter, that most distribution patterns reveal linear trends which can satisfactorily be expressed through linear regressions. The standard deviations for the sediment (x-axis) and crystalline crustal thicknesses (y-axis) do not exceed 20% of the observed thicknesses and are often considerably lower. The scatter is highest in the case of the thinned continental crust in the western Barents Sea (Fig. 3; prov. 24) where the standard deviation is 4.2 at sediment thicknesses between 0 and 15 km. Fitting the data by linear regression in this province is problematic since rifting and break-up occurred in Late Cretaceous and Eocene times and the thermal subsidence is probably not completed. Other provinces show very low scatter such as the Nordkapp Basin (prov. 10) or the basement highs off NW Novaya Zemlya (prov. 16).

The different y-axis intercepts and slopes in the different provinces (Fig. 3) provide estimates for the zero-sediment thickness and resistance to crustal thinning, respectively. Zero-sediment thicknesses range between 30 km in some provinces (e.g., prov. 17, Nordkapp Basin) to more than 45 km (e.g., prov. 14, Gardabanken High). A low slope indicates a mantle updoming below sedimentary basins (e.g., prov. 12, South Kara Basin; slope -2.0), while in

provinces with a higher slope (e.g., prov. 23, Cretaceous Volcanic Province; slope -0.7) the crust-mantle boundary is flat-lying or slightly down-warped below the sedimentary basin.

The basaltic layers of the oceanic crust in the Norwegian-Greenland Sea thin rapidly with increasing latitude while the sediment thickness decreases. Our developed model preserves very well the results of the crustal studies of Breivik et al., (2003) and Ritzmann et al. (2004) at the latitudes of Bjørnøya and northern Svalbard, respectively. The basaltic lower crustal layer 3 thins towards the north, while the upper layer 2 remains approximately constant in thickness. This suggests that magmatic activity at the oceanic spreading center is decreased with decreasing spreading rates in the narrow corridor between Eurasia and Greenland. Therefore, the traveltime through the crust and water column is about 1 sec higher in the south off the western Barents Sea (Fig. 2a).

The Barents Sea is surrounded by thick crustal complexes to the south while the crust of the Novaya Zemlya Microplate thins rapidly towards the east, indicating a transition to the Kara Sea province in the east (prov. 12), where the Moho topography is very rough and characterized by local domes (Fig. 4). These strong lateral thickness variations are well-constrained by the seismic velocity models compiled during this study (Fig. 1) and documented by the low slope in the thickness relationship of the Kara Sea province (Fig. 3).

The continental crust of northern Norway and the Kola Peninsula shows similar large thicknesses. In Fennoscandia the maximum Moho depth of 52.4 km is observed. The crustal thicknesses are also in agreement with results from unpublished receiver function analyses of the MASI99 experiment in northern Norway (Hoehne, 2001). The majority of the stations derived similar thicknesses, within a range of 1 to 3 km, to our model. Larger deviations are given in the northern coastal areas where receiver function analyses indicate shallower depth of about 40 km, where our model is founded on the FENNOLORA-experiment by Guggisberg et al. (1991) and the work of Helminsen (2002).

CONCLUSIONS AND RECOMMENDATIONS

The present study provides a new and detailed crustal velocity model, BARENTS50, for the Barents Sea region with a resolution of 50 km, and with a new compilation strategy based on geological provinces (or regionalization). Other approaches for model compilations using velocity function from seismic refraction experiments are purely based on mathematical solutions such as continuous curvature gridding or kriging methods. Other 3D models evolved from gravity modeling based on isostatic and flexural principles (e.g., Kimbell et al. 2004) or from the inversion of surface-wave dispersion data (e.g., Shapiro & Ritzwoller, 2002). The fundamental problem of all approaches, including the present one, is the non-uniqueness or ambiguity of the resulting models, which is most striking when using gravity modeling (size and shape of the anomalous body versus its density contrast). In our case, the chosen input are mostly ray tracing based models which are also ambiguous, since traveltime, layer thickness and seismic velocities are convertible parameters. Any geophysical feature of the finally constructed model (such as traveltime delays) or geological interpretation (such as the shape and extent of a lower crustal body) are naturally uncertain and, if not treated with care, can lead to false interpretations. However, the principle of layer thickness adjustments based on thickness relationships originated from the detailed analysis of the very simple but consistent dataset. The new method for adjusting the crustal thickness was particularly applicable in the Barents Sea region which is largely covered by riftogenic sedimentary basins. At this stage, it remains unclear, however, to what extent this technique is applicable to other regions worldwide. Further study is required.

Our model was already used as primary input for a new surface-wave inversion and improved, along with an extended set of recordings (Levshin et al., 2005) the mantle model comprehensively. In addition, the model provides assistance for studies of various geodynamic problems concerning the plate tectonic setting of the Barents Sea region, basin formation processes or the distribution of magmatism. Studies of the regional isostatic and thermal states and local gravity and basin modellings are backed up thanks to the availability of a complete lithosphere model.

In conclusion, the combination of a consistent seismic database and a reliable methodology to use secondary geological constraints (depth-to-basement data and thickness relations) helped significantly to establish a new higher-resolution geophysical model of the greater Barents Sea region.

REFERENCES

Bassin, C., G. Laske, and G. Masters (2000). The current limits of resolution for surface wave tomography in North America, EOS Trans. *AGU* 81: F879.

Breivik, A.J., R. Mjelde, P. Grogan, H. Shimamura, Y. Murai, and Y. Nishimura (2003). Crustal structure and transform margin development south of Svalbard on ocean bottom seismometer data, *Tectonophysics* 369: 37–70.

Faleide, J.I., E. Vagnes, and S.T. Gudlaugsson (1993). Late Mesozoic-Cenozoic evolution of the south-western Barents Sea in a regional rift-shear tectonic setting, *Mar. Petr. Geol*. 10: 186–214.

Gudlaugsson, S.T., J.I. Faleide, S.E. Johansen, and A.J. Breivik (1998). Late paleozoic structural development of the South-western Barents Sea, *Mar. Petr. Geol*. 15: 73–102.

Guggisberg, B., W. Kaminski, and C. Prodehl (1991). Crustal structure of the Fennoscandian Shield; a traveltime interpretation of the long-range FENNOLORA seismic refraction profile, *Tectonophysics* 195: 105–137.

Helminsen, L. (2002). Skorpestuktur i Finnmark og det sydvestlige Barentshav. Unpublished Master Thesis, Geological Department, University of Oslo, Oslo.

Hoehne, J. (2001). Untersuchungen der Geschwindigkeitsstruktur der Kruste und des oberen Mantels der Finnmark aus den Daten des MASI 99 Projektes. Unpublished diploma thesis, Institut für Geowissenschaften, Fachbereich Geophysik, Universitaet Potsdam, Potsdam.

Kimbell, G.F., R.W. Gadliff, J.D. Ritchie, A.S.D. Walker, and J.P. Williamson (2004). Regional three-dimensional gravity modelling of the NA Atlantic margin, *Basin Research* 16: 259–278.

Levshin, A., J. Schweitzer, C. Weidle, N. Maercklin, N. Shapiro, and M. Ritzwoller (2005). Surface wave tomography of the European Arctic, *EOS Trans. AGU* 86: (52), Fall Meet. Suppl., Abstract S51E-1053.

McKenzie, D. (1978). Some remarks on the development of sedimentary basins, *E. Planet. Sci. Let*. 40: 25–32.

Nataf, H.-C. and Y. Ricard (1996). 3SMAC: An a priori tomographic model of the upper mantle based on geophysical modeling, *Phys. Earth Planet. Inter*. 95: 101–122.

O'Leary, N., N. White, S. Tull, V. Bashiov, V. Kuprin, L. Natapov, and D. Macdonald (2004). Evolution of the Timan-Pechora and South Barents Sea basins. *Geol. Mag*. 141: (2), 141–160.

Pasyanos, M.E., W.R. Walter, M.P. Flanagan, P. Goldstein, and J. Bhattacharyya (2004). Building and testing an a priori Geophysical Model for western Eurasia and North Africa, *Pure appl. geophys*. 161: 235–281.

Ritzmann, O., W. Jokat, W. Czuba, A. Guterch, R. Mjelde, R. and Y. Nishimura (2004). A deep seismic transect in northwestern Svalbard at Kongsfjorden (Ny Ålesund) and the implications for Cenozoic break-up from Greenland: A sheared margin study. *Geophys. J. Int*. 157, 683–702.

Sakoulina, T.S., Yu. V. Roslov, and N.M. Ivanova (2003). Deep seismic investigations in the Barents and Kara seas. Rus. Acad. Sci. Physics of the Solid Earth 39: (6), 438–452.

Shapiro, N. M. and M.H. Ritzwoller (2002). Monte-Carlo inversion for a global shear velocity model of the crust and upper mantle, *Geophys. J. Int*. 151: 88–105.

Watts, A.B. (2001). Isostasy and Flexure of the lithosphere, Cambridge University Press, Cambridge, 458 pp.

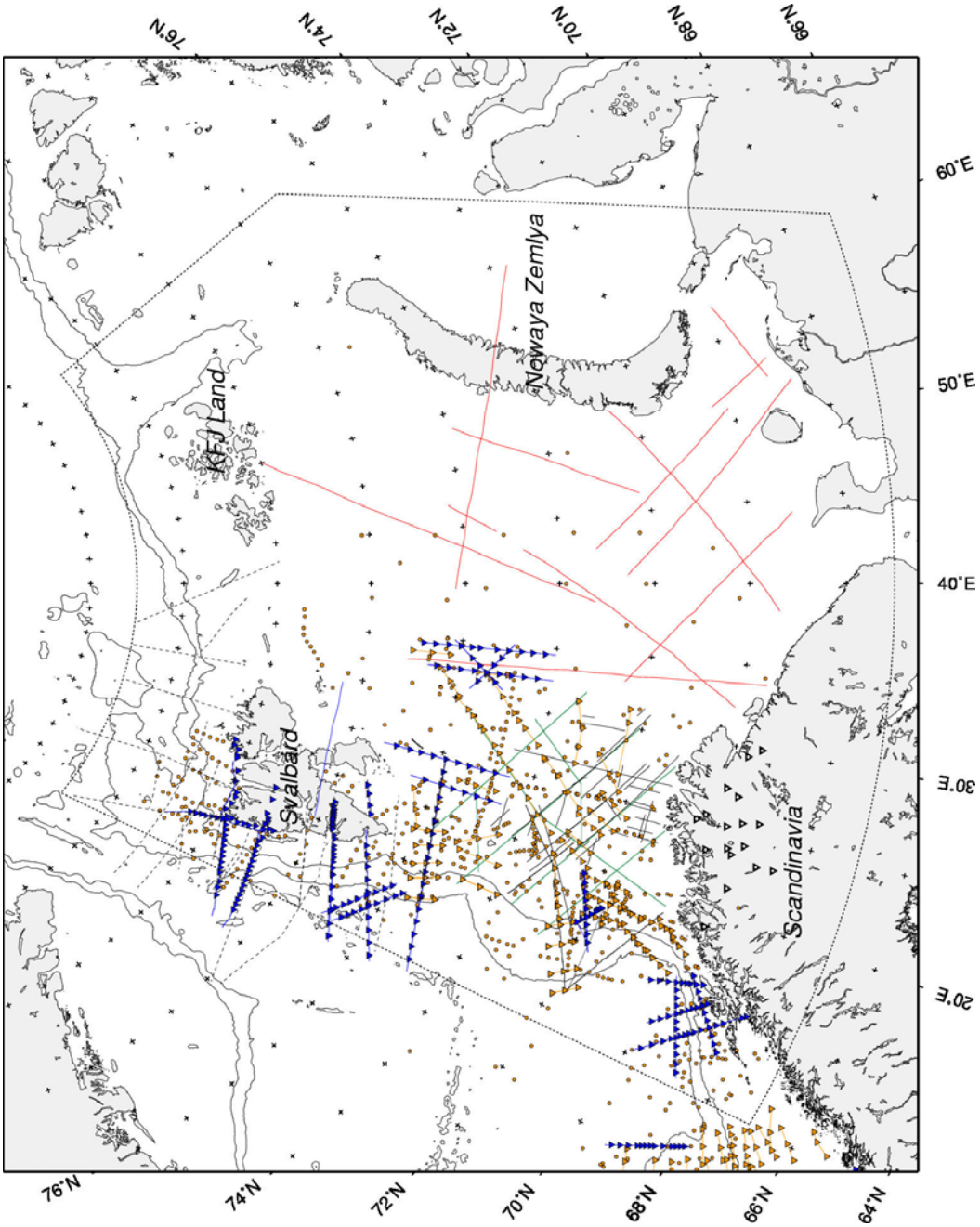

Figure 1. Location map showing principal (seismic) data coverage of the target region between Northern Scandinavia, Svalbard, Kaiser-Franz-Josef Land and Novaya Zemlya. Blue lines and blue triangles indicate deep seismic wide-angle profiles, yellow lines and yellow triangles indicate ESP profiles taken from velocity database at UiO, yellow dots indicate minor 1D-velocity profiles taken from velocity database at UiO (partly unreversed, sonarbuoys, etc.), green lines indicate IKU deep seismic MCS data that can be linked to ESP-profiles, black lines (western Barents Sea) indicate additional published MSC data, dashed lines (north and west of the Svalbard Archipelago) indicate compiled seismic transects, dotted red lines indicate MCS and wide-angle seismic lines acquired by Russian institutions and provided by MAGE (Marine Arctic Geological Expedition, Murmansk) and SMNG (Sevmorneftegeofizika: Offshore Oil and Gas Exploration, Murmansk). The bathymetry is shown with 4000, 2000 and 500 m isocontours.

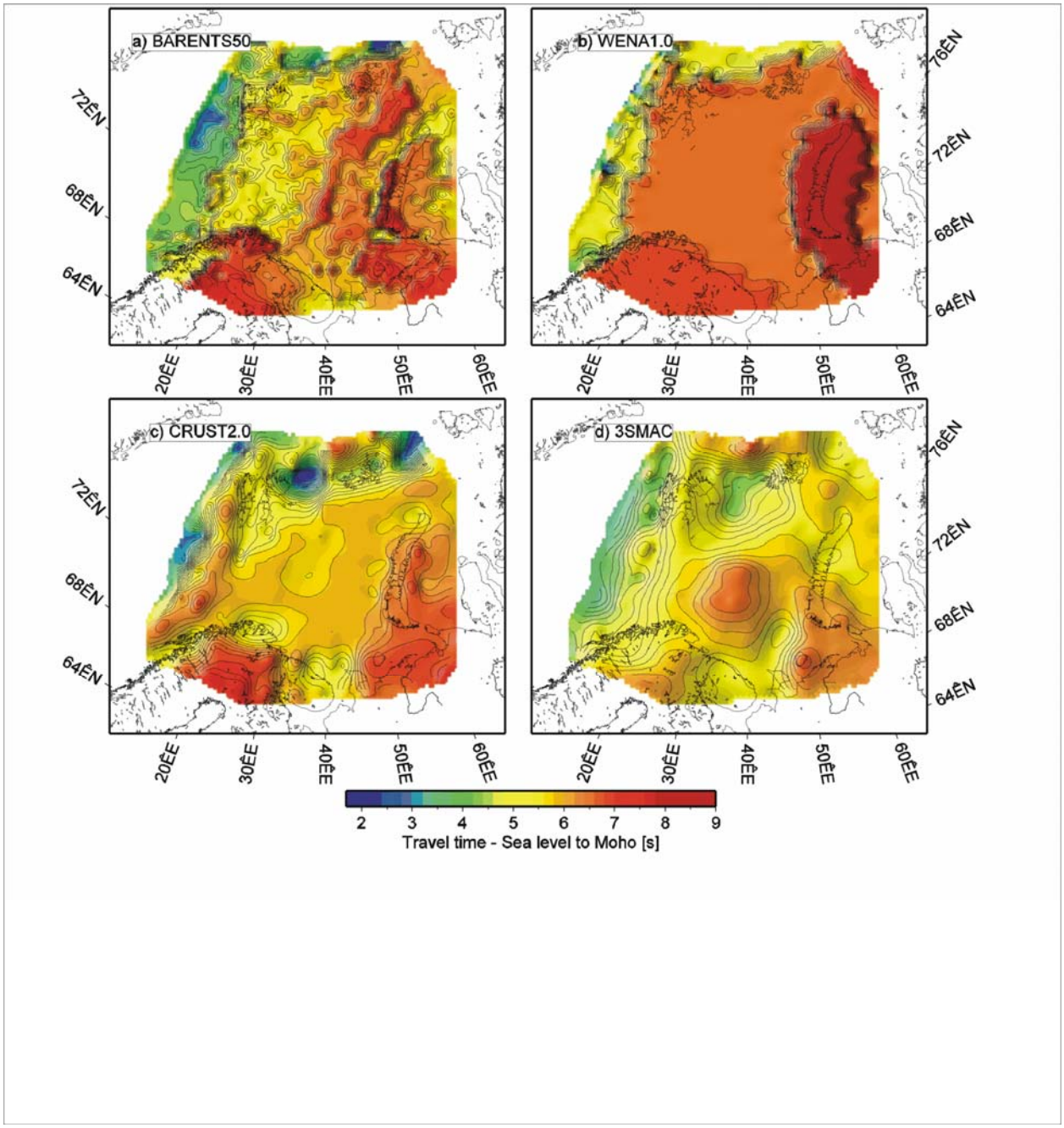

Figure 2. Traveltimes down to the Moho discontinuity. a). BARENTS50, this study. b). WENA1.0 (Pasyanos et al., 2004). c). CRUST2.0 (Bassin et al. 2000). d). 3SMAC (Nataf & Ricard 1996).

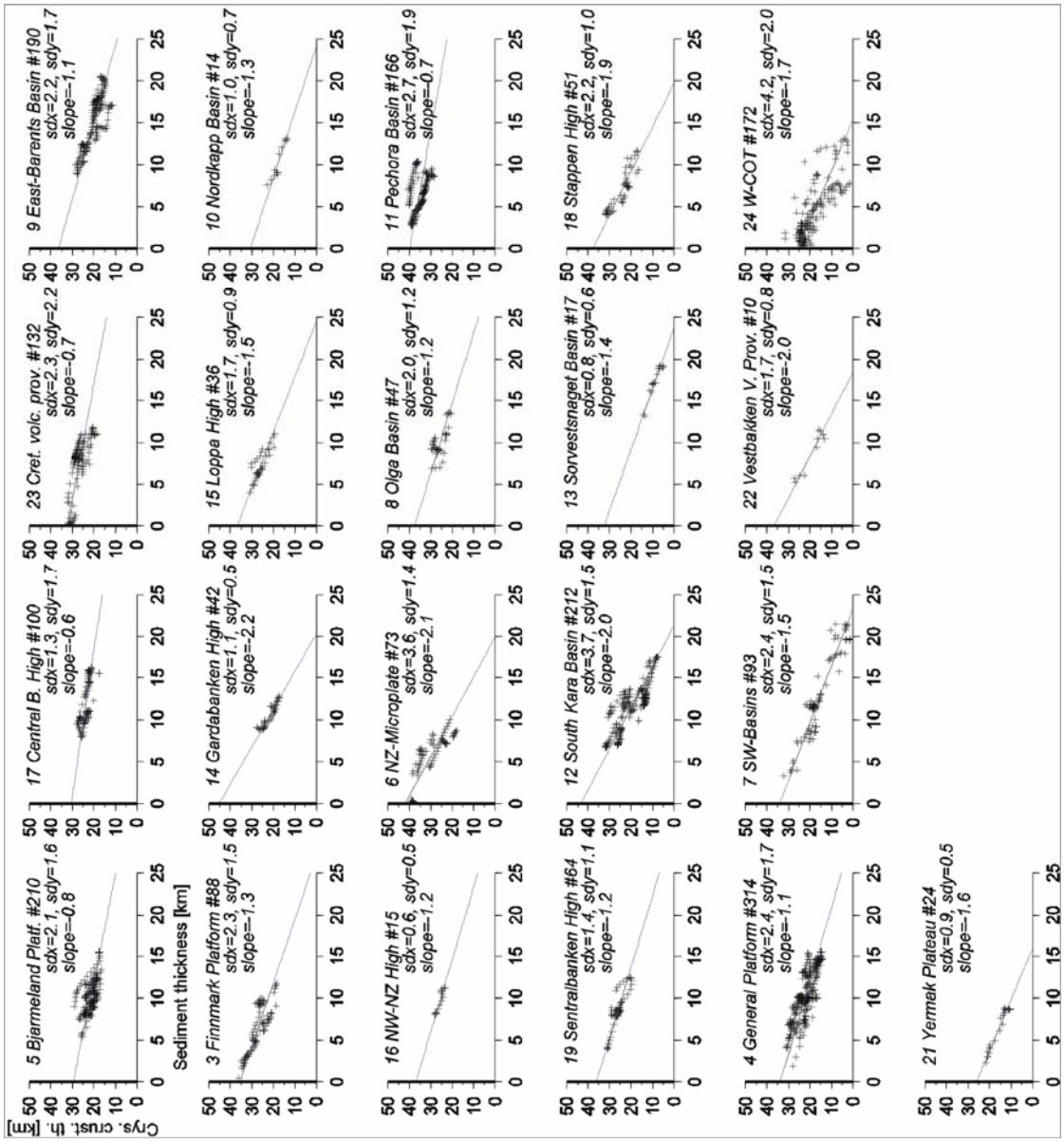

Figure 3. Sediment thickness plotted against crystalline crustal thickness for all provinces (excluding sediment-free cratons, oceanic crustal domains and regions overprinted by convergent tectonics). Black crosses are datapoints extracted from the profile database. The solid lines show the calculated linear regressions. The total number of observations is given after the #-sign. The sdx and sdy values give the standard deviations of the sediment thickness and crystalline crustal thickness, respectively.

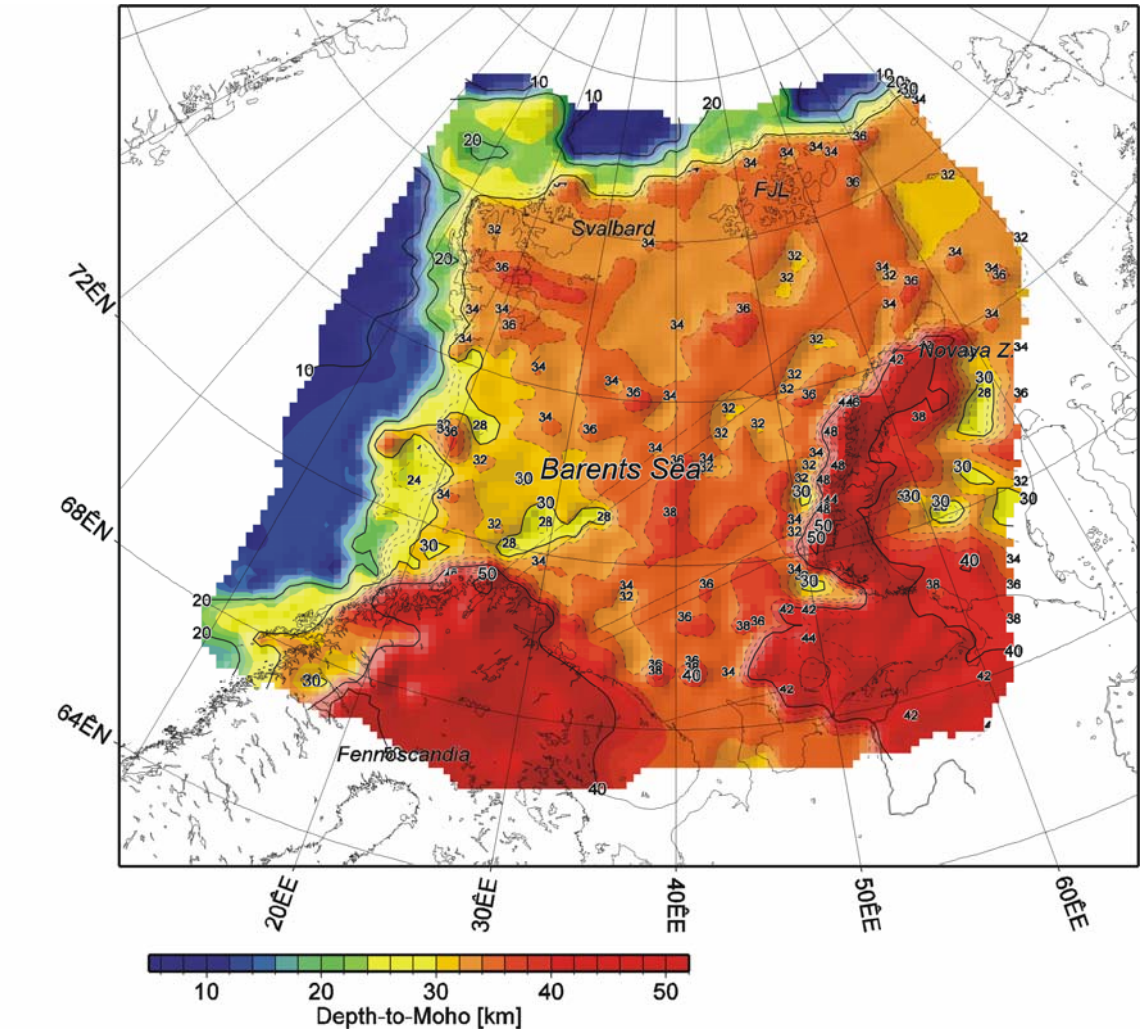

Figure 4. Depth-to-Moho from the BARENTS50 model. Provinces in the central Barents Sea, Novaya Zemlya and Kara Sea show detailed contouring (every 2 km, dashed; other contours: 10 km, solid).